

## Light-induced structural ordering of cryptochrome4 from European robin in the monomer-scale

Shigeki ARAI<sup>1\*</sup>, Rumi SHIMIZU<sup>1</sup>, Motoyasu ADACHI<sup>1</sup>,  
Hirokazu MASAI<sup>2</sup>, Koji KIMURA<sup>3</sup>, Mitsuhiro HIRAI<sup>4</sup>

<sup>1</sup>National Institutes for Quantum Science and Technology, 4-9-1 Anagwa, Inage, Chiba-city, Chiba 263-8555, Japan, <sup>2</sup>Department of Materials and Chemistry, National Institute of Advanced Industrial Science and Technology (AIST), 1-8-31 Midorigaoka, Ikeda, Osaka 563-8577, Japan. <sup>3</sup>Graduate School of Engineering Global College, Nagoya Institute of Technology, Gokiso-cho, Showa-ku, Nagoya, Aichi 466-8555, Japan, <sup>4</sup>Graduate School of Science and Technology, Gunma University, 4-2 Aramaki, Maebashi, Gunma 371-8510, Japan

### 1 Introduction

Magnetoreception, which is a sense to perceive the magnetic field information, is used for many animal behaviors (migratory, homing, feeding, breeding, etc.) [1]. Cryptochromes (CRYs), highly conserved blue light absorbing flavoproteins containing a flavin adenine dinucleotide (FAD), in retinal cells of some animal species could act as a quantum sensor to detect the angle of the geomagnetic field [2,3]. The fundamental principle of the CRY magnetosensor is that the long-lived spin-correlated radical pair (RP) generated in CRY detects the angle of the magnetic field [4]. Several spectroscopic analyses, such as transient absorption analysis near geomagnetic fields (~50  $\mu$ T), revealed that the reaction process from the composite RP to the stabilized RP proceeds over a time scale of 1 to 10  $\mu$ s [4,5]. This time scale is sufficiently longer than that required to receive geomagnetic information (approximately 1  $\mu$ s *in vivo*) [5]. The quantum yield of the stabilized RP altered by the magnetic field effect could trigger the magnetic signaling from CRY4 to the nervous system, probably through the assistance of some kinds of the conformational change accompanying with the change in the interaction to unknown CRY receptors (CRY-Rs) [6–8]. This RP mechanism, also called "CRY hypothesis", is now widely believed to be the first step in the magnetoreception process [4,6,8–10].

In this study, the structural properties of the ground state and the excited state of CRY4 from European robin (erCRY4), a representative species having the magnetoreception, were inspected by using the small-angle X-ray scattering (SAXS) method with controlling the light condition.

### 2 Experiment

The construction of erCRY4 using the *E.coli* expression system was performed by almost same procedure as previously reported [4]. Approximately a 40  $\mu$ L sample solution containing 2.7 mg/mL erCRY4, 20 mM Tris-HCl buffer (pH 8), 150 mM NaCl and 10 mM 3-mercapto-1,2-propanediol was used for SAXS measurements. The wavelength of the incident X-ray beam was 1.55 Å. The sample-to-detector distance was 1 m. To obtain the erCRY4 sample in the ground state, a tube

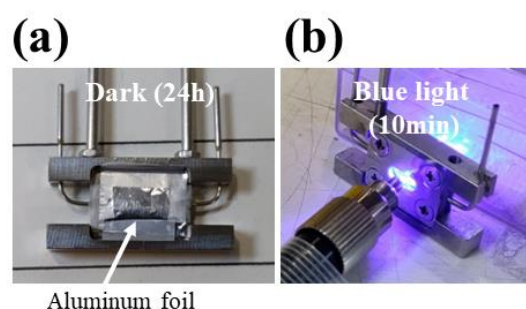


Fig. 1. Sample cells used for SAXS measurements of erCRY4 in the ground state (a) and the excited state (b).

containing erCRY4 solution was surrounded by an aluminium foil and set in the incubator (4 °C) for 24 hours before SAXS measurements.

Two different types of sample cells were used for the SAXS measurements. For the ground state measurement in the dark condition, windows of a sample cell were covered by aluminum foils in shielding ultraviolet light ~ visible light (Fig. 1a). Then the erCRY4 solution was injected into this sample cell in the darkroom. For the excited state measurement with blue light illumination, aluminum foils on windows of a sample cell were removed, and a fresh erCRY4 solution was injected into the sample cell. Then the blue LED light (wavelength: 454nm) irradiated to the erCRY4 solution for 10 min (Fig. 1b). For both the ground state and excited state measurements, background X-ray scatterings from buffer solution were also measured using the same cells as described above.

A sample cell was inserted into a cell holder at the BL-10C. The magnetic flux intensity at the sample position of BL-10C was lower than 70  $\mu$ T, which was almost same as the geomagnetic conditions. SAXS data were collected using a PILATUS3 2M detector (Detectris) at 20 °C. X-ray exposure time to collect one SAXS curve was 1 min. Buffer scattering was subtracted from each curve to yield the sample scattering curves  $I(q)$ s using the program *Sangler* [11].

After correction of the scattering data by subtracting background, the scattering curves  $I(q)$  were analyzed as

follows. The average radius of gyration ( $R_g$ ) was evaluated from  $I(q)$ s with Guinier analysis using the program *ATSAS* [12].  $I(q)$  can be approximated at the Guinier region ( $q \cdot R_g < 1.3$ ) of the scattering curves as follows:

$$I(q) = I(0)\exp(-R_g^2 q^2/3) \quad (1)$$

where  $I(0)$  denotes the intensity at  $q = 0$  and  $q$  denotes the magnitude of the scattering vector defined by the following equation:

$$q = 2\pi/d = (4\pi/\lambda) \sin(\theta/2) \quad (2)$$

where  $d$ ,  $\theta$  and  $\lambda$  are the real-space resolution, the scattering angle and the wavelength, respectively. The distance distribution function  $P(r)$  was obtained by the Fourier transform of the scattering curve  $I(q)$  as

$$P(r) = \frac{2}{\pi} \int_0^\infty r q I(q) \sin(rq) dq \quad (3)$$

where  $r$  is the real space distance.  $P(r)$  function depends on the particle shape and on the intraparticle scattering density distribution. To reduce the Fourier truncation effect in the calculation of the  $P(r)$  function, the extrapolation of the small-angle data sets using the least-squares method in the Guinier plot ( $\ln(I(q))$  vs  $q^2$ ) with the program *GNOM* [13] in the Program *PRIMUS* [12]. In this study,  $P(r)$ s were calculated from  $I(q)$ s at  $q = 0.06$ – $0.85 \text{ \AA}^{-1}$ . The maximum diameter ( $D_{max}$ ) of the particle was estimated from the  $P(r)$  function satisfying the condition  $P(r) = 0$  for  $r > D_{max}$ .

### 3 Results and Discussion

We obtained  $I(q)$ s in the  $q$ -range of  $0.06$ – $0.85 \text{ \AA}^{-1}$  for both the ground state and the excited state, which mainly reflect information of the tertiary structure and intramolecular structure of erCRY4 in the real spatial resolution  $d=7$ – $105 \text{ \AA}$  (Fig. 2a).  $I(q)$  profiles were slightly different between the ground state and the excited state.  $R_g$ s estimated by eq. (1) were  $26 \text{ \AA}$  for the ground state and  $25 \text{ \AA}$  for the excited state, respectively.

$I(q)$ s were further converted to  $P(r)$ s (Fig. 2b).  $D_{max}$  of the excited state ( $73 \text{ \AA}$ ) was smaller than that of the ground state ( $77 \text{ \AA}$ ), while the peak height of the excited state was slightly higher than that of the ground state, indicating that the  $P(r)$  profile of erCRY4 was changed to a more symmetrical bell shape upon blue light illumination. This result suggests that, at the erCRY4 monomer scale, the tertiary structure was contracted and the molecular shape became more globular in the excited state than in the ground state.

Moreover, to inspect the structural properties of erCRY4 in detail, we predicted molecular models of the erCRY4 monomer using the program *SREFLEX* [14] with the X-ray crystal structures of erCRY4 homologous proteins PDB: 3FY4 (sequence identity 44.8%) and PDB: 6PU0 (sequence identity 87.9%) as templates. The *SREFLEX* program uses normal mode analysis in Cartesian space to estimate the flexibility of high-resolution models of biological macromolecules and improve their agreement with experimental SAXS data [14]. By using the *SREFLEX* program, molecular models with high consistency with the experimental  $I(q)$ s at  $q=0.06$ – $0.5 \text{ \AA}^{-1}$  were predicted (Fig. 2c and 2d). The

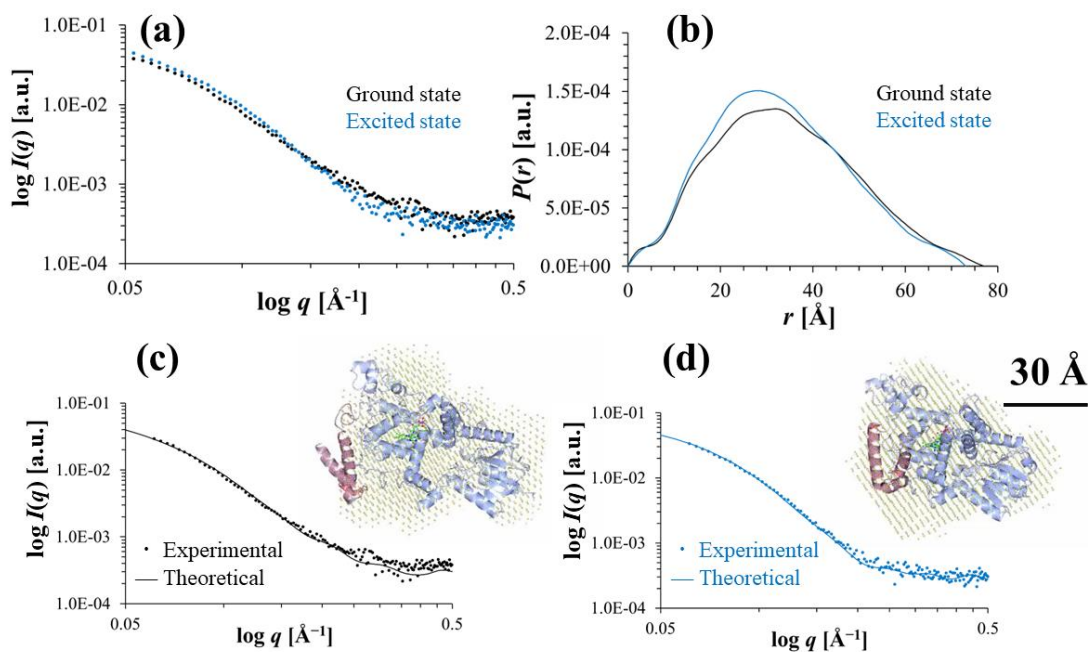


Fig. 2. Results of SAXS analyses for erCRY4. (a) Experimental scattering curves  $I(q)$ s. (b)  $P(r)$ s obtained from  $I(q)$ s shown in (a). (c) and (d) show results of *SREFLEX* analyses for the ground state and the excited state, respectively. Ribbon models show the tertiary structures of erCRY4 predicted by *SREFLEX* analyses. Red chains in the models shown in (c) and (d) indicate the C-terminal regions.

discrepancies (chi-squared values) between the experimental  $I(q)$ s and the theoretical  $I(q)$ s of molecular models predicted by *SREFLEX* were 2.07 for the ground state and 1.71 for the excited state. The molecular model in which the tertiary structure was slightly expanded and the C-terminal region leaved from the FAD binding domain was predicted as the optimal structure for the ground state (Fig. 2c), while the molecular model in which the tertiary structure contracted and the C-terminal region approached the FAD binding domain was predicted as the optimal structure for the excited state (Fig. 2d). These results suggest that the blue light illumination causes not only the RP formation but also the light-induced structural ordering of erCRY4 in the monomer-scale. The specific tertiary structure upon light illumination may be a key of signaling magnetic field effects to neurons. Related to this study, we are currently investigating the structural properties of CRY-R candidates, such as iron-sulfur cluster assembly 1 (ISCA1), potassium voltage-gated channel subfamily V member 2 (KCNV2), etc., and the effect of interaction with CRY-R on the structural order of CRY (2024G026). In addition, we are currently working on multifaceted structural analysis, including SAXS measurements in the lower  $q$ -range and electron magnetic resonance (EPR), because blue light illumination is known to cause dimerization of erCRY4 [15].

#### Acknowledgement

This work was supported by JSPS KAKENHI [grant numbers 18K06174, 21K06093, 21K14581, 23H04125, 23K17662] and MEXT Quantum Leap Flagship Program (MEXT Q-LEAP) [grant number JPMXS0120330644 and 20206207]. Synchrotron radiation experiments were performed at the BL-10C of Photon Factory (Proposal Nos. 2022G003 and 2024G026) and at the BL01B1, BL14B2 and BL44B2 of SPring-8 (Proposal Nos. 2023B1936, 2023B1046 and 2023B1131). This work was partially conducted in Institute for Molecular Science, supported by “Advanced Research Infrastructure for Materials and Nanotechnology in Japan (ARIM)” of the Ministry of Education, Culture, Sports, Science and Technology (MEXT). Proposal Number JPMXP1223MS1094.

#### References

- [1] Johnsen S & Lohmann KJ. *Nat Rev Neurosci* **6**, 703–712 (2005).
- [2] Ritz T, Adem S & Schulten K. *Biophysical Journal* **78**, 707–718 (2000).
- [3] Mouritsen H & Ritz T. *Current Opinion in Neurobiology* **15**, 406–414 (2005).
- [4] Xu J, *et al.*, *Nature* **594**, 535–540 (2021).
- [5] Maeda K, *et al.*, *Proc Natl Acad Sci USA* **109**, 4774–4779 (2012).
- [6] Otsuka H, *et al.*, *Biochemistry* **59**, 3615–3625 (2020).
- [7] Watari R, *et al.*, *Journal of Biological Chemistry* **287**, 42634–42641 (2012).
- [8] Cintolesi F, *et al.*, *Chemical Physics* **294**, 385–399 (2003).
- [9] Maeda K, *et al.*, *Nature* **453**, 387–390 (2008).

- [10] Hore PJ & Mouritsen H, *Annu Rev Biophys* **45**, 299–344 (2016).
- [11] Shimizu N, *et al.*, *AIP Conference Proceedings* **1741**, 050017 (2016).
- [12] Manalastas-Cantos K, *et al.*, *J Appl Crystallogr* **54**, 343–355 (2021).
- [13] Svergun DI, *Journal of Applied Crystallography* **25**, 495–503 (1992).
- [14] Panjkovich A & Svergun DI, *Phys Chem Chem Phys* **18**, 5707–5719 (2016).
- [15] Hanić M, *et al.*, *J Phys Chem B* **127**, 6251–6264 (2023).

\* arai.shigeki@qst.go.jp